

PCCP

Accepted Manuscript



This is an *Accepted Manuscript*, which has been through the Royal Society of Chemistry peer review process and has been accepted for publication.

Accepted Manuscripts are published online shortly after acceptance, before technical editing, formatting and proof reading. Using this free service, authors can make their results available to the community, in citable form, before we publish the edited article. We will replace this *Accepted Manuscript* with the edited and formatted *Advance Article* as soon as it is available.

You can find more information about *Accepted Manuscripts* in the [Information for Authors](#).

Please note that technical editing may introduce minor changes to the text and/or graphics, which may alter content. The journal's standard [Terms & Conditions](#) and the [Ethical guidelines](#) still apply. In no event shall the Royal Society of Chemistry be held responsible for any errors or omissions in this *Accepted Manuscript* or any consequences arising from the use of any information it contains.

Reduction Mechanisms of Additives on Si Anodes of Li-Ion Batteries

Julibeth M. Martínez de la Hoz and Perla B. Balbuena*

Department of Chemical Engineering and Department of Materials Science and Engineering
Texas A&M University, College Station, TX 77843

* e-mail: balbuena@tamu.edu

2nd revision submitted to Phys. Chem. Chem. Phys., June 18, 2014

Abstract

Solid-electrolyte interphase (SEI) layers are films deposited on the surface of Li-ion battery electrodes during battery charge and discharge processes. They are due to electrochemical instability of the electrolyte which causes electron transfer from (to) the anode (cathode) surfaces. The films could have a protective passivating role and therefore understanding the detailed reduction (oxidation) processes is essential. Here density functional theory and ab initio molecular dynamics simulations are used to investigate the reduction mechanisms of vinylene carbonate (VC) and fluoroethylene carbonate (FEC) on lithiated silicon surfaces. These species are frequently used as “additives” to improve the SEI properties. It is found that on lithiated Si anodes (with low to intermediate degrees of lithiation) VC may be reduced via a $2 e^-$ mechanism yielding an opened VC^{2-} . At higher degrees of lithiation, such species receives two extra electrons from the surface resulting in adsorbed $CO_2^{2-}_{(ads)}$ anion and a radical anion $\cdot OC_2H_2O^{2-}$. Additionally, in agreement with experimental observations, it is shown that CO_2 can be generated from reaction of VC with the CO_3^{2-} anion, a product of the reduction of the main solvent, ethylene carbonate (EC). On the other hand, FEC reduction on Li_xSi_y surfaces is found to be independent of the degree of lithiation, and to occur through three mechanisms. One of them leads to adsorbed VC^{2-} anion upon release from the FEC molecule and adsorption on the surface of F^- and one H atom. Thus in some cases, the reduction of FEC may lead to the exact same reduction products as that of VC, which explains similarities in SEI layers formed in presence of these additives. However, FEC may be reduced via two other multi-electron transfer mechanisms, that result in formation of either CO_2^{2-} , F^- , and $\cdot CH_2CHO^-$, or CO^{2-} , F^- , and $\cdot OCH_2CHO^-$. These alternative reduction products may oligomerize and form SEI layers with different components to those formed in the presence of VC. In all cases, FEC reduction also

leads to formation of LiF moieties on the anode surface, in agreement with reported experimental data. The crucial role of the surface in each of these mechanisms is thoroughly explained.

1. Introduction

Despite advances in lithium-ion battery research, the technology still does not meet current energy density requirements for high-end portable electronics and hybrid electric vehicles.¹⁻³ Silicon anode-based batteries have higher theoretical capacities than those obtained with graphitic anodes, but they do not retain their capacity for prolonged cycles due to dramatic volume changes of the silicon anode during lithiation/delithiation cycles.⁴⁻⁷ Current studies focus on proposing alternatives to improve the long cycle life of this anode material. Among them, the use of slight amounts of additives in the electrolyte has been considered. Several experimental works have demonstrated the positive effect of electrolyte additives on electrochemical performance, thermal stability, and structure retention of silicon anodes.⁸⁻¹⁵ Some of the most commonly used additives are fluoroethylene carbonate (FEC) and vinylene carbonate (VC), which are structural modifications of ethylene carbonate (EC) with a C=C bond (VC) or with a fluorine atom (FEC). Silicon electrodes cycled in the presence of VC or FEC show enhanced capacity retention, a more stable cycling efficiency, and an overall lower resistivity to transport Li⁺ ions, compared to those electrodes cycled with no additives.⁸⁻¹⁵ These improvements in electrochemical performance are associated with the different chemical structure and morphology of solid electrolyte interphase (SEI) layers formed on silicon surfaces due to electrolyte reduction at the anode surface. For example, capacity retention of silicon electrodes may be related to homogeneous SEI layers that experience less severe morphological changes during cycles, hindering cracking and isolation of portions of the active Si-phase.¹¹⁻¹⁵ A lower charge-transfer resistance may be linked to thinner surface films reported in the presence of FEC and VC,^{11,12,14} and also to a unique different chemical structure of their SEI layers that may facilitate the transport of Li⁺ ions.^{8,9,11-15} Flexible polymeric species are found to be the main component of SEI layers formed in the presence of these additives, and interestingly, these polymeric species are not observed in electrodes cycled using only typical EC, DEC, and LiPF₆ electrolyte components.^{8,9,11,12,14,15}

Chemical characterization of FEC- and VC-derived SEI layers have been performed mostly using X-ray photoelectron spectroscopy (XPS) and Fourier transformed infrared spectroscopy

(FTIR). In the case of XPS, a unique peak at 534.5 eV in the O-1s spectrum, has been associated exclusively to the presence of polymeric compounds.^{16,17} This peak has been detected for electrodes cycled in the presence of FEC¹¹ and also in those cycled in the presence of VC⁹, which suggest the presence of similar polymeric compounds in FEC- and VC-derived SEI layers. Regarding FTIR measurements, a group of peaks around 1800 cm⁻¹ corresponding to polycarbonate species has only been detected when VC and FEC are present in the electrolyte.^{8,9,11,14,15} Chen et al¹⁴ and Dalavi et al⁹ observed these peaks when using VC as additive, whereas Nie et al¹⁵ and Etacheri et al¹¹ observed them while using FEC. Despite similarities observed in VC- and FEC-derived SEI layers, some important differences between them have also been indicated. For instance, the concentration of LiF in FEC-derived SEI layers is much higher than that of SEI layers obtained in FEC-free electrolytes.^{8,11-13,15} On the other hand, SEI layers obtained in VC-containing electrolytes have a much lower LiF concentration compared to those in additive-free solutions.^{9,14} LiF is a stable compound with high binding energy that can maintain a stable interface and provide prolonged stability to the SEI layer.^{8,13} However, its lower proportion in VC-derived layers suggests that the main factor needed to obtain a stable, homogeneous SEI layer, is the presence of flexible organic polymeric compounds.

However, it is yet not clear how these polymeric compounds are formed or their exact chemical structure. It has been proposed they are either poly-alkenes, poly-carbonates,¹⁵ or polyene compounds.¹² Also, they are thought to originate from polymerization of VC or VC-reduction products through the double bond.^{14,16,18,19} In fact, this theory can be coupled with suggestions by Aurbach et al^{11,20} and Winter et al⁸ of FEC undergoing elimination of HF and forming VC. This may explain similarities in the composition of SEI layers derived from these additives. However, the mechanism of FEC and VC reduction on Silicon anodes is yet not clear, and the elimination of HF from FEC has not been proved. Given the direct relation between chemical composition of SEI layers and the electrochemical performance of the electrode, it is important to elucidate the mechanisms of FEC and VC reduction on silicon anodes and the different reduction products originated in each case.

In this work we use density functional theory (DFT) and ab-initio molecular dynamics calculations (AIMD) to elucidate the most favorable reduction mechanisms of VC and FEC on

silicon anodes. In the past, we have utilized these types of calculations to determine reduction mechanisms of ethylene carbonate (EC) on silicon anodes at different degrees of lithiation (LiSi_4 , LiSi_2 , LiSi , and $\text{Li}_{13}\text{Si}_4$),²¹ EC and FEC reductions at ultra-low degrees of Si lithiation²², and also the reduction of FEC on $\text{Li}_{13}\text{Si}_4$ surfaces.²³ Here we focus on determining the most favorable reduction mechanisms for VC and FEC as a function of Si anode lithiation (LiSi_2 , LiSi , and $\text{Li}_{13}\text{Si}_4$), and we discuss the main similarities and/or differences between the reduction products found in each case. Additionally, we propose a pathway for the formation of CO_2 from VC, a gas that is detected when electrodes are cycled in the presence of this additive.¹⁶

2. Computational and system details

2.1. Investigation of VC and FEC reduction mechanisms

Reduction mechanisms of FEC and VC molecules on lithiated silicon anodes are studied by simulating liquid FEC-EC and VC-EC mixtures in contact with a lithiated Si electrode. The modelled lithiation stages correspond to LiSi_2 , LiSi , and $\text{Li}_{13}\text{Si}_4$. Crystallographic and electronic information of the unit cells representing these surfaces can be found in our previous work (For the LiSi concentration, only the $\text{LiSi}(101)\text{-O}$ and $\text{LiSi}(101)\text{-OH}$ systems were used).²¹ In each case, the number of EC molecules in contact with the electrode was chosen as to represent the density of their liquid phase (1.32 g/cm^3). Subsequently, three of these EC molecules were replaced by three FEC or VC molecules, and a molecular dynamics minimization was performed using the consistent valence force field (CVFF) as implemented in the DISCOVER simulation software.²⁴ CVFF is considered good for modeling small organic crystals and gas phase structures.²⁵ For the minimization a smart algorithm was used combining steepest descent, conjugate gradient, and Newton methods. The maximum force among all the atoms in the system required for convergence was set to $0.001 \text{ kcal mol}^{-1} \text{ \AA}^{-1}$. The minimized geometry obtained was then used as the initial configuration for the AIMD simulations. The number of EC and FEC/VC molecules in contact with each Li_xSi_y surface is shown in Table 1.

Table 1 Number of EC and FEC/VC molecules used to model the liquid phase in contact with each Li_xSi_y surface. The total number of molecules reproduces the density of EC in liquid phase (1.32 g/cm^3)

Li_xSi_y surface	Number of FEC or VC molecules	Number of EC molecules	wt% of FEC (VC)
LiSi_2	3	7	34 (30)
LiSi	3	10	27 (23)

Li ₁₃ Si ₄	3	9	29 (25)
----------------------------------	---	---	---------

The concentrations (wt%) of the additives used in the simulations are much higher compared to those used in experiments (usually < 5%). However, this does not affect the simulated behavior of the nascent stages of reduction, where the key interaction is that of the molecule with the electrode material.

2.2. Investigation of reaction pathways for the formation of CO₂ from VC

In order to explain the release of CO₂ gas during cycling of silicon anodes in the presence of VC, a series of spontaneous reactions between VC and EC-reduction products are proposed and tested. In our previous work, we reported EC⁻, EC²⁻, CO₃²⁻, and ·OC₂H₄O²⁻ anions to be the main reduction products of EC found in liquid phase.²¹ In this work, possible spontaneous reactions between these anions and VC are studied by AIMD simulations of specific VC-X species immerse in EC-liquid phase (X: EC⁻, EC²⁻, CO₃²⁻, and ·OC₂H₄O²⁻). In every case, the system consisted of a cubic cell with dimensions a=b=c=11.3Å. Periodic boundary conditions were applied in the x, y, and z-directions. The density in the cell corresponded to that of liquid EC (1.32 g/cm³), with 13 EC molecules and the corresponding VC-X species. A molecular dynamics minimization was performed to every system, prior to the AIMD simulations, with parameters indicated in the previous section.

Each of the VC-X species was optimized in gas phase, previous to the AIMD simulation, to ensure using the most stable configuration. The optimized VC-X species investigated are shown in Figure 1. If the proposed VC-X product (X: EC⁻, EC²⁻, CO₃²⁻, and ·OC₂H₄O²⁻) was found to spontaneously separate during the DFT optimization, it was concluded that the reaction was not favorable. This was only observed in the cases of VC-EC⁻, as observed in Figure 1 (E and F). In all other cases, the VC-X moieties remained forming a complex (A, B, C, D, G, and H). These VC-X complexed species were immersed in liquid EC and studied through AIMD simulations to evaluate possible further reactions in the electrolyte. Figure 2 shows an example of the initial configuration for the AIMD simulation of species D (Figure 1) immersed in liquid EC.

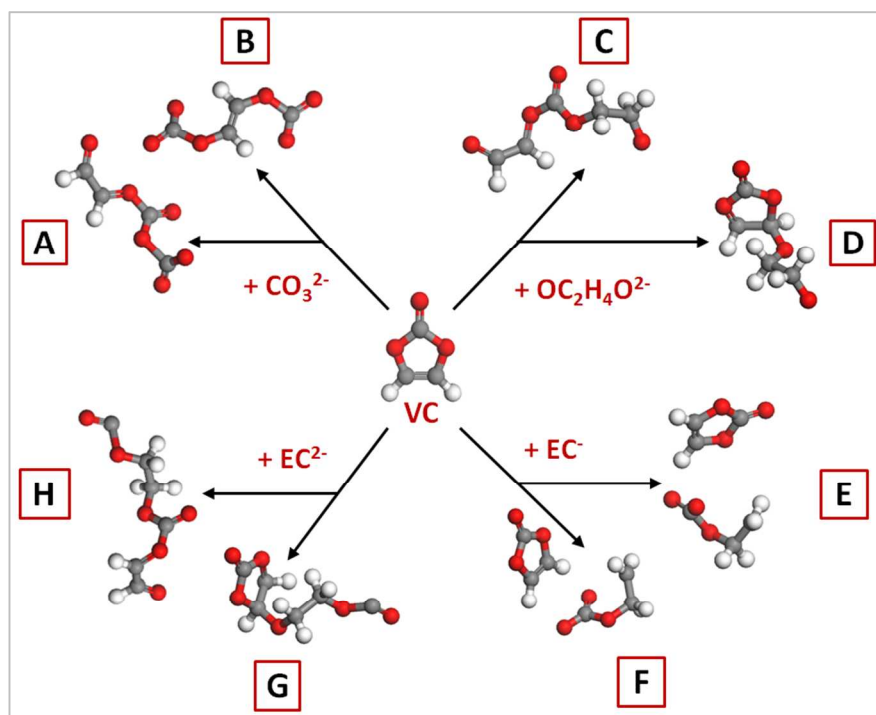


Figure 1. A-H represent different optimized VC-X species used to study possible spontaneous reactions between VC and EC-reduction products, including CO_3^{2-} , $\text{OC}_2\text{H}_4\text{O}^{2-}$, EC^- , and EC^{2-} . In each case the added anion reactant attacks the carbonyl carbon (A, C, E, and H) or the ethylene carbon (B, D, F, and G) of the VC molecule. In cases E and F the VC-X complex separated during the DFT optimization, and in A, B, C, and H, one of the C-O bonds of the VC molecule was broken. Color code: O is red, H is white, and C is black.

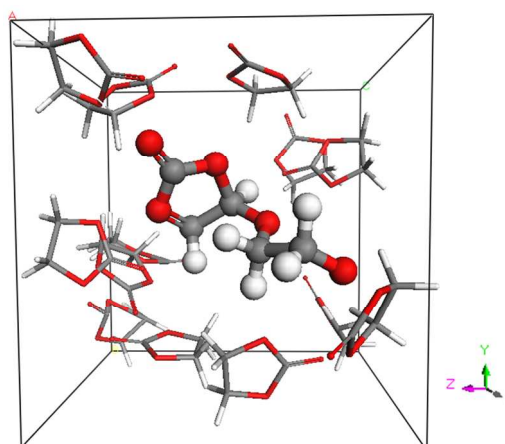


Figure 2. Initial configuration for the AIMD simulation of the $\text{VC}\cdot\text{OC}_2\text{H}_4\text{O}^{2-}$ species (D in Figure 1) immerse in liquid EC. $\text{VC}\cdot\text{OC}_2\text{H}_4\text{O}^{2-}$ molecules are represented as ball-stick. Color code as in Figure 1.

2.3. General computational details

Calculations were performed using the Vienna ab initio simulation package VASP,²⁶⁻³⁰ with the Perdew-Burke-Ernzerhof functional (GGA-PBE)³¹ and the projector augmented wave (PAW) pseudopotentials provided in the VASP databases describing electron-ion interactions.^{32,33} AIMD simulations were carried out using the NVT ensemble at 450 K and a time step of 1 femtosecond. Tritium masses are substituted for protons to permit this time step. The Nose thermostat was used to control the temperature oscillations during the simulation with a Nose-mass parameter of 0.5, which gives a frequency of oscillation corresponding to 176 time steps. A Γ -point Brillouin zone sampling was applied in this case with a planewave energy cutoff of 400 eV. In the case of VC/FEC reductions, two different initial configurations of the liquid phase were used for each of the Li_xSi_y surfaces studied, to account for randomness of the liquid phase. All of the systems were allowed to run enough time to observe spontaneous reduction of FEC and VC molecules on the Li_xSi_y surfaces, or reaction between the VC molecule and the EC-reduction products (more than 8 picoseconds in every case).

Bader charge analyses were used to perform charge calculations.^{16,17} Within this method, the total electronic charge of an atom is approximated by the charge enclosed within the Bader volume defined by zero flux surfaces. Additionally, calculations of activation energies for dissociation of some adsorbates (Section 3.1) were performed using the nudged elastic band (NEB) method.³⁴⁻³⁶ The method works by optimizing a number of intermediate images along the reaction path on the potential energy surface, while the initial and the final images corresponding to the reactant and product, respectively, are optimized previous to the NEB calculation. Convergence criteria for optimizations are set to 10^{-3} and 10^{-4} eV, for ionic relaxation loop and electronic self-consistent iteration, respectively. A Gaussian smearing with a width of 0.05 eV was employed and a $4 \times 4 \times 1$ k-points Monkhorst-Pack³⁷ mesh sampling was used in the surface Brillouin zone.

3. Results

3.1. VC reduction mechanisms on Li_xSi_y surfaces

Charge analyses shown in Figure 3 allowed the determination of average partial atomic charges on the VC and FEC molecules in liquid-phase. Significant charge distribution is observed in both

molecules. For VC, the largest partial charges are on the oxygen atoms and the carbonyl C_1 atom, corresponding to approximately $-1.0|e|$ and $+2.0|e|$, respectively. This marked charged distribution is consistent with the population analysis reported by Ushirogata et al. for VC in liquid EC.³⁸ Charges of Si and Li atoms in the different Li_xSi_y surfaces were calculated in our previous work.²¹ In general, the charge of Li^+ ions is $+0.83|e|$ and that of Si atoms vary with the lithiation of the surface. Silicon atoms in the $LiSi_2$ surface have an average charge of $-0.41|e|$; those in the $LiSi$ surface have charges between -0.80 and $0.0|e|$ (depending on their coordination state to other Si atoms), whereas those in the $Li_{13}Si_4$ surface bear charges between -2.0 and $-3.2|e|$. Thus, differences in reduction mechanisms may be possible.

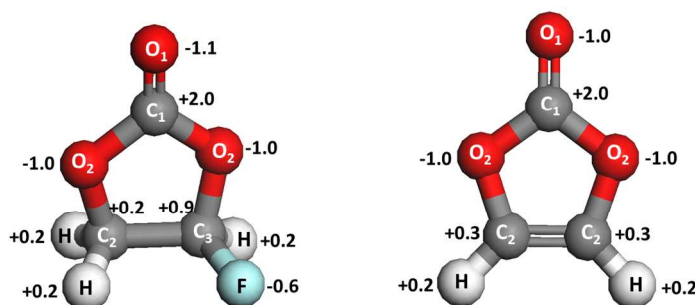


Figure 3. Average partial Bader atomic charges calculated for FEC molecules (left) and VC molecules (right) in the liquid phase in contact with Li_xSi_y surfaces. Color code: C is black, O red, H white, and F light blue.

In all of the studied surfaces ($LiSi_2$, $LiSi$, and $Li_{13}Si_4$), the adsorption of VC starts with electrostatic interactions between the negatively charged carbonyl oxygen O_1 of the molecules and Li^+ ions on the anode surface (Figure 4a), which allows some of the molecules to get closer to the surface and finally become adsorbed through the formation of a C_1 -Si bond (Figure 4b). However, the amount of charge transferred to the molecule upon adsorption depends on the degree of lithiation of the silicon anode. At relatively *low lithium concentrations*, $LiSi_2$ and $LiSi$, the VC molecule receives two electrons, which causes the breaking of a C_1 - O_2 bond on the adsorbed molecule and the formation of the VC opened radical anion $\cdot OC_2H_2OCO^{2-}_{(ads)}$ species (Figure 4c). Ushirogata et al. also found the cleavage of the C_1 - O_2 bond to be favored during the one- and two-electron reductive decomposition of VC in liquid EC.³⁸ They suggested that the fragility of this bond is related to a strong π -conjugation of the O_2 - C_2 - C_2 - O_2 moiety in the VC anion molecule, which disfavors large structural changes in the C_2 - O_2 bond. Reaction (1)

describes the reduction pathway followed by VC molecules adsorbing on LiSi_2 and LiSi surfaces.



We note that the one-electron reduction yielding $\cdot\text{OC}_2\text{H}_2\text{OCO}^-$ (opened VC $^-$) may happen only in ultra-low lithiated Si surfaces as found for EC²², where the geometry of adsorbed Li in contact with the solvent or additive molecule may be close to the simulated geometry for reduction in liquid phase.³⁸ As soon as Li is alloyed with Si, Li atoms are no longer adsorbed *over the surface* plane but they are distributed *on the surface or subsurface*. This alternative geometry allows Li atoms to easily interact with the carbonyl O of the solvent or additive, which gets adsorbed to the surface via a strong C-Si bond thus favoring a fast two-electron reduction. Moreover, on the *higher lithiated* $\text{Li}_{13}\text{Si}_4$ surface, the first step of VC reduction also takes place through the two-electron mechanism described by reaction (1), with transference of charge between a Si-atom on the surface and the C_1 atom in the VC molecule during its adsorption. However, upon adsorption of the molecule on the surface (Figure 4b) and breaking of the first $\text{C}_1\text{-O}_2$ bond (Figure 4c), *two additional electrons* are transferred to the adsorbed anion after a few hundred femtoseconds. This additional electron transfer was detected by following the evolution of the VC electronic charge as a function of the $\text{C}_1\text{-Si}$ distance, as shown in our previous work for EC reduction on lithiated Si surfaces.²¹ This triggers the breaking of a second $\text{C}_1\text{-O}_2$ bond and generates $\text{CO}^{2-}_{(\text{ads})}$ and $\cdot\text{O}(\text{C}_2\text{H}_2)\text{O}^{2-}$ as reduction products. The latter may go to the liquid phase, as described in reaction (2) and Figure 4d. This additional electron transfer may be also observed on lower lithiated silicon surfaces, but it is much less frequent. Out of six different simulations of VC reducing on LiSi_2 and LiSi surfaces in only one of them reaction (2) was detected, whereas in the other five only reaction (1) was observed. Ushirogata et al. studies in liquid phase (no surface included) also reported the formation of $\cdot\text{O}(\text{C}_2\text{H}_2)\text{O}^-$ and CO (gas) during the two-electron reductive decomposition of VC-Li^+ . They showed that the breaking of the second $\text{C}_1\text{-O}_2$ bond in the VC anion stabilizes the $\text{O}_2\text{-C}_2\text{-C}_2\text{-O}_2$ moiety by recovering its symmetric conjugation.³⁸



Reduction products in (1) and (2) were the only ones observed upon adsorption of VC on Li_xSi_y surfaces, and were also found by Ushirogata et al. for the calculated reduction of VC in liquid phase;³⁸ however the opened VC^- product found in liquid phase is not obtained in lithiated Si surfaces. In addition, no direct formation of CO_2 was detected. Thus, in order to estimate activation barriers required to obtain CO and CO_2 from the opened VC radical anion $\cdot\text{OC}_2\text{H}_2\text{OCO}^{2-}_{(\text{ads})}$ in (1), these barriers were calculated in gas-phase for $\cdot\text{OC}_2\text{H}_2\text{OCO}^{2-}$ adsorbed on a $\text{LiSi}(101)\text{-H}$ surface. Optimized configurations along the reaction coordinates, and their energies, can be found as supplementary information (Fig. S1). Calculated activation barriers correspond to 0.54 and 2.0 eV for the formation of CO and CO_2 , respectively. Even though our transition state calculation does not take into account the liquid phase surrounding the adsorbed $\cdot\text{OC}_2\text{H}_2\text{OCO}^{2-}$ radical anion, the significant difference in barriers may explain why the formation of CO_2 is not observed in the AIMD simulations. Detectable amounts of CO_2 gas have been found during cycling of electrodes in VC-containing electrolytes.¹⁶ However, our calculations suggest that this gas does not come *directly* from reduction of VC on the Li_xSi_y electrode, but it may rather be produced as a result of *reactions of VC with EC-reduction products* present in the liquid phase, as it will be discussed in the next section.

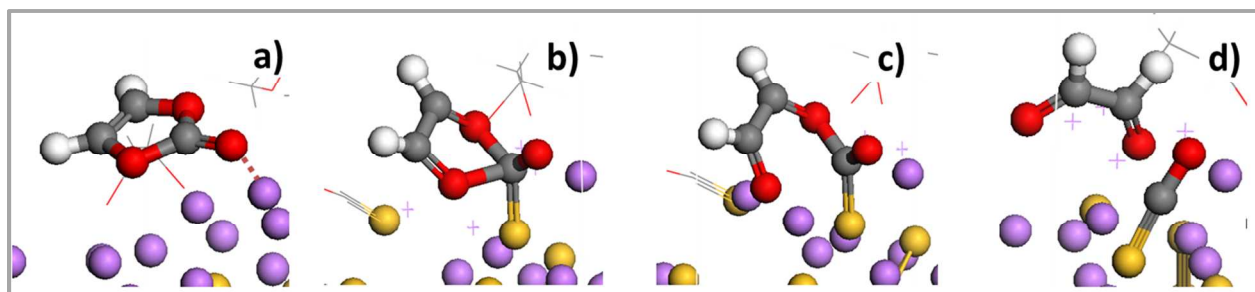


Figure 4. Reduction of VC on a $\text{Li}_{13}\text{Si}_4\text{-010}$ surface. **(a)** VC adsorption starts with electrostatic interaction between the negatively charged carbonyl oxygen O_1 of the molecule and Li^+ ions on the surface **(b)** A $\text{C}_1\text{-Si}$ bond is formed **(c)** Upon adsorption and transference of two-electrons from the surface to the molecule a $\text{C}_1\text{-O}_2$ bond is broken. The resultant adsorbed species is an opened VC anion with a double negative charge. **(d)** The cleavage of a second $\text{C}_1\text{-O}_2$ bond is observed upon transference of two additional electrons to the adsorbed VC anion. Color code: Li is purple, Si yellow, O red, C black, and H white.

3.1.1. Investigation of spontaneous reactions between VC and EC-reduction products

AIMD simulations of VC-X species immerse in liquid EC revealed that spontaneous formation of CO_2 from VC is possible. Species E and F (Figure 1) were found to spontaneously separate

during the DFT optimization. In cases B, C, and D, no changes were observed in the VC-X species during 8-ps of AIMD simulation. However, in cases A, G, and H, further changes in the VC-X species were observed, resulting in reactions described in (3), (4), and (5), respectively:



Reaction (3) shows spontaneous formation of CO_2 as a result of VC reacting with the CO_3^{2-} anion. This anion is expected to be present in the liquid electrolyte as a result of the reductive decomposition of EC at the solid/electrolyte interface on lithiated Si anodes, as shown in our previous work.¹⁹ Consequently, even though direct formation of CO_2 is not observed from the reduction of VC on lithiated silicon surfaces, it is still possible to release this gas when VC reacts with some reduction products of the EC solvent. We note that Ushirogata et al.³⁸ proposed a different alternative for CO_2 production arising from attack of intact VC by EC^- anion radicals. The proposal is attractive because it may explain the role of VC as suppressor of further EC reduction thus inducing a smaller irreversible capacity due to SEI formation in presence of VC. However our previous analysis illustrated that the *one electron* reduction of EC is one of the two possible mechanisms in low²² to intermediate lithiated surfaces (LiSi_4 , LiSi_2 , and LiSi) and it is much less frequently observed on highly lithiated Si surfaces ($\text{Li}_{13}\text{Si}_4$)¹⁹. Therefore we postulate that while the mechanism proposed by Ushirogata et al. may be operative at higher potentials (before Li intercalation) or low lithiation stages, the above discussed reaction (3) for CO_2 production from VC should be a much feasible pathway on both intermediate and higher lithiated Si-anodes.

3.2. FEC reduction mechanisms on Li_xSi_y surfaces

Charge analyses allowed the determination of average partial atomic charges on the FEC molecules in liquid-phase. These charges are reported in Fig. 3 (left). A significant charge distribution is also observed in FEC molecules, with the largest partial charges on the oxygen atoms and the C_1 atom, corresponding to approximately $-1.0|e|$ and $+2.0|e|$, respectively. In addition, differences in the charges of carbon atoms C_2 and C_3 are observed ($+0.2|e|$ and $+0.9|e|$,

respectively) due to the bonding of C₃ to the electronegative fluorine atom. This distributed charge is consistent with the high polarity of FEC that has a dielectric constant (relative to vacuum) close to 110 at room temperature. As in the case of VC, the adsorption process on the Li_xSi_y surfaces starts with electrostatic interactions between the negatively charged O₁ of the FEC molecule and Li⁺ ions on the anode, and ends up with the formation of a C₁-Si bond (J in Fig. 5). However, in this case the amount of charge transferred to the FEC molecule upon adsorption is found to be *independent of the degree of lithiation* of the silicon surface. This is attributed to its high electron affinity revealed by its reduction potential (1.63V) compared with those of EC (1.36V) and VC (1.40 V). Three different reduction mechanisms are observed in all three Li_xSi_y surfaces studied (I, II, and III in Figure 5). In I and II, a total of *four* electrons are transferred to the FEC molecule, which may result in either decomposition into CO₂²⁻, F⁻, and ·CH₂CHO⁻ or into CO₂²⁻, F⁻, and ·OCH₂CHO⁻. In mechanism III, a total of *three* electrons are transferred, resulting in the formation of the ·OC₂H₂OCO²⁻ species, which corresponds to the adsorbed VC²⁻ anion represented in Fig. 4(c) and reaction (1). Formation of VC from FEC through the release of HF was suggested earlier by Aurbach et al^{11,18} and Winter et al⁸, as mentioned in the introduction. However, up to now, there was no proof of the FEC molecule undergoing such reaction. Mechanisms I, II, and III are discussed in more detail below.

All of the calculated FEC reduction mechanisms are depicted in Figure 5. They start with transfer of two electrons from the surface to the adsorbed FEC molecule, causing the cleavage of one C₁-O₂ bond (In some cases, the highly reactive Li₁₃Si₄ surface also transfers electrons to nearby *non-adsorbed* FEC molecules). Breaking of the C₁-O₂ bond has been reported as the most favorable step during the two-electron reduction of an FEC molecule on Li(Si₁₅H₁₆) clusters²², and during the reduction of an FEC⁻ anion in the presence of dielectric continuum simulating the electrolyte environment of the battery²³. This first reduction step is represented by reaction (6), and the resulting adsorbed molecule (opened FEC anion radical) is shown in Figure 5 (species K). Almost simultaneously, a fluoride anion leaves the molecule and is adsorbed on the lithiated surface, leaving the adsorbed ·OC₂H₃OCO⁻ species on the silicon anode (L in Fig. 5), and taking one of the electrons from the opened FEC anion radical. This is reaction (7). The F⁻ interacts with Li⁺ ions on the electrode at distances around 1.8 Å, which is slightly longer than reported experimental Li-F distances (1.56 Å)³⁹ and may be a precursor to the nucleation of an amorphous LiF film formed on these Li_xSi_y surfaces. This type of reaction derived from FEC molecules

explains the larger concentration of LiF detected experimentally in the presence of FEC additive.^{8,11-13,15} This is in agreement with findings by Lucht et al, who previously demonstrated that FEC can be a source of LiF.¹⁵



Figure 5 (K and L) illustrates two modes of adsorption of opened FEC: in K the fluorine atom points towards the solution whereas in L it points to the surface. Starting from L, the surface may transfer two more electrons to the adsorbed anion, which may result in the breaking of a C₂-O₂ bond forming CO₂²⁻_(ads) and ·CH₂CHO⁻, if pathway I is followed (reaction 9). Otherwise, another C₁-O₂ bond is broken, forming CO²⁻_(ads) and ·OCH₂CHO⁻ (pathway II, and reaction 8). Pathway I was observed by Leung et al. during the AIMD simulation of a FEC-EC mixture in contact with Li₁₃Si₄, and pathway II was proposed by the same authors as the most favorable for the one-electron reduction of the FEC molecule in liquid phase.²³ Our AIMD simulations show that either pathway, I or II, may be followed upon transference of two additional electrons to species L. Additionally, a third important reaction happens when one of the H atoms in L is in the proximity of a surface silicon atom. In such case an H-Si bond may be formed, resulting in the ·OC₂H₂OCO⁻ fragment (VC anion with a single negative charge, pathway III, and reaction 10). After a few additional hundred femtoseconds of simulation, the Li_xSi_y surface transfers one more electron to this adsorbed anion, which becomes the adsorbed VC²⁻ anion depicted in Figure 4(c). As discussed in section 3.1, this VC²⁻ anion may dissociate into CO²⁻_(ads) and ·OC₂H₂O²⁻ on highly lithiated surfaces. Transformation of FEC to VC anion upon release of H and F atoms may explain similarities in the polycarbonate species detected when using VC and FEC additives in the electrolyte.^{8,9,11,14,15}

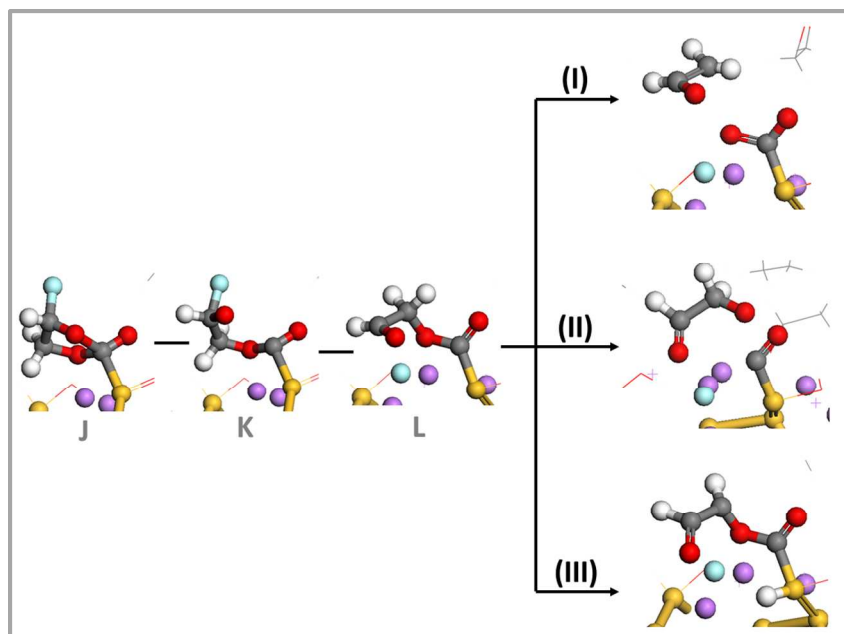


Figure 5. FEC reduction mechanisms observed on Li_xSi_y surfaces



The results of this section show the large variety of reduction products obtained upon reduction of FEC on lithiated silicon surfaces. Reduction pathway III leads to the same reduction products obtained from VC decomposition on Li_xSi_y anodes, explaining similarities observed in FEC- and VC-based SEI layers. However, FEC may undergo two other reduction pathways (I and II), which result in charged fragments $\cdot\text{OC}_2\text{H}_3\text{O}^-$ and $\cdot\text{C}_2\text{H}_3\text{O}^-$. These anions may go to the liquid phase and attack intact solvent molecules in the electrolyte generating oligomer-type products different from those obtained through VC. Another important difference identified for SEI layers being generated in the presence of FEC, is the formation of Li-F films from reduction of fluorine atoms leaving FEC molecules. All of these results agree with experimental observations of the chemical structure of SEI layers formed in the presence of FEC and VC additives. Thus, identification of detailed reduction mechanisms of electrolyte components is essential to explain specific characteristics of SEI layers formed in silicon anodes. Moreover, this discussion highlights the crucial role of the surface on the reduction mechanisms of solvents and additives.

4. Conclusions

Reduction mechanisms for VC and FEC additives were identified as a function of the degree of lithiation of the silicon anode using static DFT and AIMD simulations. In the case of VC, a two-electron mechanism was observed at the lower lithiation stages (LiSi_2 and LiSi), which results in an adsorbed VC^{2-} anion with a broken $\text{C}_1\text{-O}_2$ bond. Two more electrons are transferred to this species at the higher lithiated $\text{Li}_{13}\text{Si}_4$ surface, which generates $\text{CO}_2^{2-}(\text{ads})$ and $\cdot\text{OC}_2\text{H}_2\text{O}^{2-}$. Although no direct formation of CO_2 is observed upon reduction of VC on Li_xSi_y surfaces, spontaneous reactions between VC and EC-reduction species revealed that CO_2 can be released upon reaction of VC with the CO_3^{2-} anion, present in the liquid phase of the electrolyte after reduction of the solvent EC. This is an alternative mechanism to the one proposed recently³⁸ where CO_2 is produced via reaction of VC with EC^- . Our simulations suggest that the one electron reduction of EC is much less frequent on Si surfaces at intermediate or higher stages of lithiation, where our proposed mechanism should be prevalent.

Due to its high reactivity, reduction of FEC on Li_xSi_y surfaces was found to be extremely fast, independent of the degree of lithiation, and able to proceed through three different mechanisms. One of them leads to the adsorbed VC^{2-} anion upon release of H and F atoms from the FEC molecule. This is a very interesting finding showing that in some cases the reduction of FEC and VC leads to the exact same reduction products, and explaining similarities in SEI layers formed in the presence of these additives. However, FEC molecules can be also reduced through two other mechanisms, involving the sequential transference of four electrons to the molecules and resulting in either formation of CO_2^{2-} , F^- , and $\cdot\text{CH}_2\text{CHO}^-$ or CO^{2-} , F^- , and $\cdot\text{OCH}_2\text{CHO}^-$. These latter reduction products, which are different to the ones produced from VC reduction, may oligomerize and form SEI layers with different components to that formed in the presence of VC. Additionally, in every FEC decomposition pathway observed, the fluorine atom leaves the FEC molecule being reduced and forming LiF moieties on the anode surface. This is in agreement with experimental observation of increased LiF concentration on SEI layers formed in the presence of FEC.

Results obtained in this work agree with features observed by experimental reports of chemical structure of SEI layers formed in the presence of FEC and VC additives. This demonstrates that detailed studies of reduction mechanisms of different components of the electrolyte can be used

to elucidate the formation process of SEI layers on silicon anodes. Future work will focus on analyzing further reaction and/or polymerization of FEC and VC reduction products.

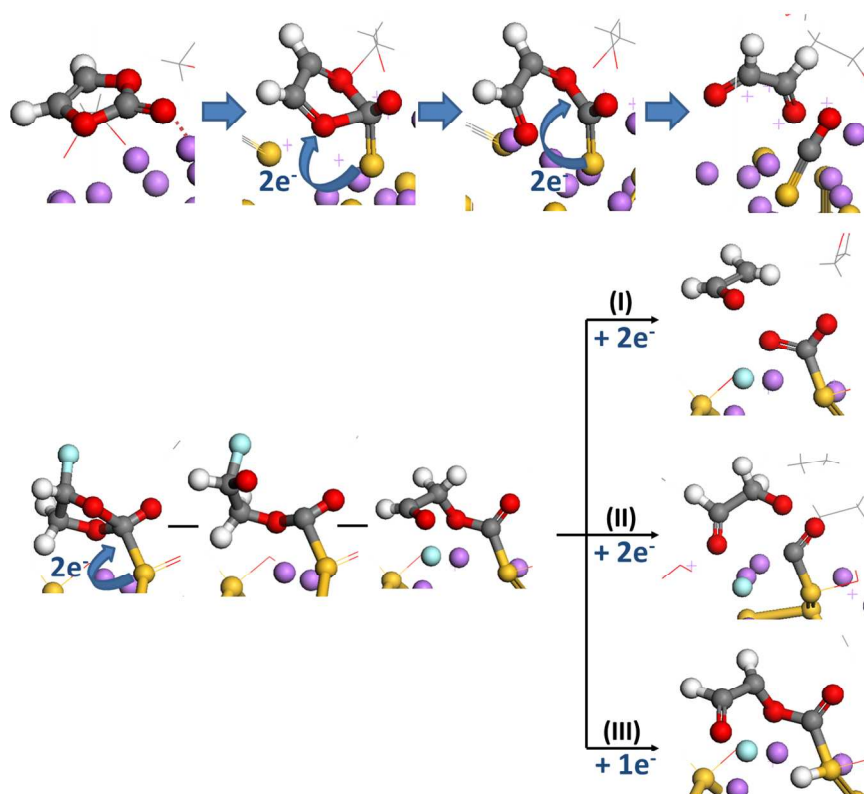
Acknowledgements. This work was supported by the Assistant Secretary for Energy Efficiency and Renewable Energy, Office of Vehicle Technologies of the U.S. Department of Energy under Contract No. DE-AC02-05CH11231, Subcontract No. 7060634 under the Batteries for Advanced Transportation Technologies (BATT) Program. Computational resources from Texas A&M Supercomputing Center, Brazos Supercomputing Cluster at Texas A&M University and from Texas Advanced Computing Center at UT Austin are gratefully acknowledged.

References

- (1) Armand, M.; Tarascon, J. M.: *Nature* 2008, **451**, 652-657.
- (2) Choi, N.-S.; Chen, Z.; Freunberger, S. A.; Ji, X.; Sun, Y.-K.; Amine, K.; Yushin, G.; Nazar, L. F.; Cho, J.; Bruce, P. G.: *Angewandte Chemie International Edition* 2012, **51**, 9994-10024.
- (3) Goodenough, J. B.; Kim, Y.: *Chemistry of Materials* 2009, **22**, 587-603.
- (4) Zhang, W.-J.: *Journal of Power Sources* 2011, **196**, 13-24.
- (5) Raimann, P. R.; Hochgatterer, N. S.; Korepp, C.; Möller, K. C.; Winter, M.; Schröttner, H.; Hofer, F.; Besenhard, J. O.: *Ionics* 2006, **12**, 253-255.
- (6) Hatchard, T. D.; Dahn, J. R.: *Journal of The Electrochemical Society* 2004, **151**, A838-A842.
- (7) Zhang, X.-W.; Patil, P. K.; Wang, C.; Appleby, A. J.; Little, F. E.; Cocke, D. L.: *Journal of Power Sources* 2004, **125**, 206-213.
- (8) Profatilova, I. A.; Stock, C.; Schmitz, A.; Passerini, S.; Winter, M.: *Journal of Power Sources* 2013, **222**, 140-149.
- (9) Dalavi, S.; Guduru, P.; Lucht, B. L.: *Journal of The Electrochemical Society* 2012, **159**, A642-A646.
- (10) Lin, Y.-M.; Klavetter, K. C.; Abel, P. R.; Davy, N. C.; Snider, J. L.; Heller, A.; Mullins, C. B.: *Chemical Communications* 2012, **48**, 7268-7270.
- (11) Etacheri, V.; Haik, O.; Goffer, Y.; Roberts, G. A.; Stefan, I. C.; Fasching, R.; Aurbach, D.: *Langmuir* 2011, **28**, 965-976.
- (12) Nakai, H.; Kubota, T.; Kita, A.; Kawashima, A.: *Journal of The Electrochemical Society* 2011, **158**, A798-A801.
- (13) Choi, N.-S.; Yew, K. H.; Lee, K. Y.; Sung, M.; Kim, H.; Kim, S.-S.: *Journal of Power Sources* 2006, **161**, 1254-1259.
- (14) Chen, L.; Wang, K.; Xie, X.; Xie, J.: *Journal of Power Sources* 2007, **174**, 538-543.
- (15) Nie, M.; Abraham, D. P.; Chen, Y.; Bose, A.; Lucht, B. L.: *The Journal of Physical Chemistry C* 2013, **117**, 13403-13412.
- (16) Ota, H.; Sakata, Y.; Inoue, A.; Yamaguchi, S.: *Journal of The Electrochemical Society* 2004, **151**, A1659-A1669.

- (17) El Ouatani, L.; Dedryvère, R.; Siret, C.; Biensan, P.; Gonbeau, D.: *Journal of The Electrochemical Society* 2009, **156**, A468-A477.
- (18) Wang, Y.; Nakamura, S.; Tasaki, K.; Balbuena, P. B.: *J. Am. Chem. Soc.* 2002, **124**, 4408-4421.
- (19) Wang, Y. X.; Balbuena, P. B.: *J. Phys. Chem. B* 2003, **107**, 5503-5510.
- (20) Aurbach, D.; Gamolsky, K.; Markovsky, B.; Gofer, Y.; Schmidt, M.; Heider, U.: *Electrochimica Acta* 2002, **47**, 1423-1439.
- (21) Martinez de la Hoz, J. M.; Leung, K.; Balbuena, P. B.: *ACS Applied Materials & Interfaces* 2013, **5**, 13457-13465.
- (22) Ma, Y.; Balbuena, P. B.: *J. Electrochem. Soc.* 2014, **161**, E3097-E3109.
- (23) Leung, K.; Rempe, S. B.; Foster, M. E.; Ma, Y.; Martinez del la Hoz, J. M.; Sai, N.; Balbuena, P. B.: *Journal of The Electrochemical Society* 2014, **161**, A213-A221.
- (24) Materials Studio v5 5.0.0. Accelrys Software Inc, 2010.
- (25) Song, C.; Wu, W.; Al-Ostaz, A.: Effects of Force Field in Molecular Mechanics Simulation of Geo-Materials. In *GeoCongress 2008*; American Society of Civil Engineers, 2008; pp 1012-1019.
- (26) Kresse, G.; Furthmüller, J.: *Physical Review B* 1996, **54**, 11169-11186.
- (27) Kresse, G.; Furthmüller, J.: *Computational Materials Science* 1996, **6**, 15-50.
- (28) Kresse, G.; Hafner, J.: *Physical Review B* 1993, **48**, 13115-13118.
- (29) Kresse, G.; Hafner, J.: *Physical Review B* 1993, **47**, 558-561.
- (30) Kresse, G.; Hafner, J.: *Physical Review B* 1994, **49**, 14251-14269.
- (31) Perdew, J. P.; Burke, K.; Ernzerhof, M.: *Physical Review Letters* 1996, **77**, 3865-3868.
- (32) Blöchl, P. E.: *Physical Review B* 1994, **50**, 17953-17979.
- (33) Kresse, G.; Joubert, D.: *Physical Review B* 1999, **59**, 1758-1775.
- (34) Henkelman, G.; Jonsson, H.: *The Journal of Chemical Physics* 2000, **113**, 9978-9985.
- (35) Henkelman, G.; Uberuaga, B. P.; Jonsson, H.: *The Journal of Chemical Physics* 2000, **113**, 9901-9904.
- (36) Sheppard, D.; Terrell, R.; Henkelman, G.: *The Journal of Chemical Physics* 2008, **128**, 134106-10.
- (37) Monkhorst, H. J.; Pack, J. D.: *Physical Review B* 1976, **13**, 5188-5192.
- (38) Ushirogata, K.; Sodeyama, K.; Okuno, Y.; Tateyama, Y.: *Journal of the American Chemical Society* 2013, **135**, 11967-11974.
- (39) DeFrees, D. J.; Levi, B. A.; Pollack, S. K.; Hehre, W. J.; Binkley, J. S.; Pople, J. A.: *Journal of the American Chemical Society* 1979, **101**, 4085-4089.

Table of Contents Graphic



Lithiated Si anodes facilitate reduction of carbonate additives through multiple electron transfers